Received: 12 September 2024 | Accepted: 20 February 2025 | Published: 10 March 2025

DOI: 10.1111/1365-2435.70054

BRITISH ECOLOGICAL SOCIETY Functional Ecology

RESEARCH ARTICLE

Betting on rains that do not co area overshoot relate to increa

Kelly L. Kerr[1,2] | Leander D. L. Anderegg[2] | Trevor Keenan[3] | William R. L. Anderegg[1,4]

[1]School of Biological Sciences, University of Utah, Salt Lake City, Utah, USA

[2]Department of Ecology, Evolution, and Marine Biology, Univ Santa Barbara, California, USA

[3]Department of Geography, University of California, Santa Barbara, California, USA

[4]Wilkes Center for Climate Science and Policy, University of Utah, Salt Lake City, Utah, USA

Correspondence
Kelly L. Kerr
Email: klkerr86@gmail.com

Funding information
David and Lucille Packard Foundation; Blavatnik Family Foundation; Alan T. Waterman Award, Grant/Award Number: IOS-2325700; National Science Foundation, Grant/Award Number: 1802880, 2003017, 2003205, 2044937 and 2216855; USDA Agriculture and Food Research Initiative, Grant/Award Number: 1027700; Gordon and Betty Moore Foundation, Gra GBMF11974

Handling Editor: Tamir Klein

Abstract

1. Structural overshoots, where biomass is overallocated to tree leaf area compared to sapwood area, could result in lethal stress during droughts. Climate change may alter climatic cues that drive leaf area production, such as temperature and precipitation, as well as seasonal dynamics that underlie summer rainfall due to the North American Monsoon (NAM). Combined matches between leaf area-driven water demand and availability, and increased drought-induced mortality events.
2. We used leaf area to sapwood area ratios to investigate the prevalence of overshoots and whether overshoots increase drought-induced mortality. We measured populations of aspen spanning the no during and following severe droughts.
3. We observed increased overshoots and drought-induced mortality in southern latitude populations that rely more on summer monsoon rainfall. Changes in convective activity from low snowpack the preceding winter may be a climatic driver of heightened summer monsoon rainfall in the region and therefore may also trigger increased production of leaf area during wetter summers.
4. Our results suggest that an overshoot of leaf area to sapwood area (A_L:A_S) ratios is associated with drought-induced tree mortality and highlight that climate-change driven alterations to the NAM could species' acclimation to environmental change.

KEYWORDS
aspen, climate change, drought, leaf area to sapwood area, mortality, North American monsoon, *Populus tremuloides*

1 | INTRODUCTION

Shifts in biomass allocation between leaf area (A_L), which reflects hydraulic demand, and sapwood area (A_S), which reflects hydraulic supply capacity, are a primary way that tree species limit water loss due to increased evaporative demands during drought periods. Both between- and within-species variation in the ratio of A_L:A_S occurs in predictable ways (i.e. reduced A_L in arid climates), and adjustments

in A_L:A_S in response to environmental change typically occur on intermediate time scales (i.e. during a growing season or across a few years), making it a key drought response functional trait (Anderegg et al., 2021; DeLucia et al., 2000; Gleason et al., 2013; Lachenbruch et al., 2021; Martínez-Vilalta et al., 2009; Mencuccini, 1995; Rosas et al., 2019; Trugman et al., 2019). However, temporal mismatches between water demand and availability can result in maladaptation to environmental conditions, resulting in 'structural overshoot' where trees construct too much leaf (i.e. evaporating) area during wet periods relative to the sapwood area that can supply water to the canopy and then consequently desiccate during periods of drought (Jump et al., 2017; Zhang et al., 2021).

Climate change may alter relationships among climate factors, such as seasonal coupling between temperatures and snowpack with summer monsoonal rainfall, which could have major implications for the ability of tree species to acclimate to rapid environmental change. In the southwestern United States (sensu Seager et al., 2007), the North American Monsoon (NAM) delivers more than half of the region's annual rainfall (Adams & Comrie, 1997) and provides a critical source of water for many tree species. Climate model simulations have documented that NAM rainfall is anticipated to increase in the future, driven by snowpack and temperatures whereby low snowpack tends to trigger increased convective activity and stronger monsoonal rainfall (Notaro & Zarrin, 2011; Zhu et al., 2005). Yet a recent study of land-atmosphere coupling patterns has documented a weakening NAM signal under current climate change, leading to more variable summer precipitation patterns in the future and a decoupling of the feedback between winter snowpack and summer monsoonal precipitation, referred to as the 'NAM Shift' (Kerr et al., 2017). Climate change is also likely to lead to more low snowpack years (Ashfaq et al., 2013), which, combined with monsoonal failure, could be lethal for southwestern forests. If trees are not able to acclimate to these shifting climatic regimes, they could trigger structural overshoot in forests in response to highly fluctuating climate signals, increasing tree mortality risk and reducing water availability in forest stands.

Extensive drought-induced tree mortality of forests has occurred in recent decades, particularly in the southwestern United States (Anderegg et al., 2012; Bell et al., 2014; Williams et al., 2020). Given the potential weakening of drought resistance that provides >50% of the water for a majority of forests in the southwestern US, understanding functional trait responses and mismatches that influence drought mortality risk remains a critical area of research for forecasting future forest mortality patterns (Trugman et al., 2021). Previously documented relationships between specific leaf area (SLA, leaf area divided by mass) and mortality raise the possibility that trait mismatches with hydraulic supply could drive mortality (Greenwood et al., 2017). A_L:A_S may also influence tree mortality following drought, as higher A_L:A_S heightens evaporative demand and reduces supply capacity during periods of lower water availability. A mismatch between supply and demand could occur at the tissue scale or the stand scale, yet the scaling of branch-level to stand-level A_L:A_S remains a crucial unknown for leveraging tree traits to predict forest drought vulnerability (Mencuccini et al., 2019).

Allometric equations provide tools for estimating stand-level leaf area from sapwood area measurements (Eagleson, 1982; Marshall & Waring, 1986; Shinozaki et al., 1964; Waring et al., 1982; Whitehead et al., 1984). Sperry et al., 2019), and more ecologically relevant understandings of forest stand structure, resource competition, and tree response to stress. Therefore, a critical but untested hypothesis is that structural overshoot and maladaptive variations in branch- and stand-level A_L:A_S (more leaf area or evaporative demand than available water supply) accelerate forest mortality during severe drought events.

We tested the hypothesis that maladaptive variations in A_L:A_S might accelerate forest mortality within and across populations of aspen (*Populus tremuloides*), a widespread and ecologically important tree species in North America that has experienced drought stress and regional drought-driven mortality over the past two decades (Anderegg et al., 2013; Worrall et al., 2008). These populations span the northern transition zone of the NAM across temperature and precipitation gradients. We asked: (1) How does A_L:A_S (both branch- and stand-level) vary across temporal and spatial gradients? (2) Do climate correlations provide a mechanism for leaf production patterns in monsoon-dependent populations of aspen, and (3) is leaf area structural overshoot linked to increased mortality risk from drought?

2 | METHODS

We quantified aspen leaf area dynamics following severe drought in 2018 and 2020 across five natural populations of aspen within National Forests (NF) that span the northern transition zone of the NAM in the United States. These included the Dixie NF, White River NF and Uinta NF (Figure 1a). The southernmost populations (e.g. Dixie and San Juan) typically experience the greatest NAM precipitation, while the northern latitude forests (e.g. White River and Uinta) receive the least NAM precipitation. We also intensively studied leaf area dynamics in the San Juan NF across elevation and through meteorologically disparate years (2014, 2018, 2019, 2020).

In recent decades, all populations of aspen in the southwestern US have experienced drought stress, which is reflected by Palmer Drought Severity Index (PDSI) values (Figure 1b). During the severe drought years of 2018 and 2020, PDSI values across the sampled populations ranged from −3 to −5 and from −2 to −6 (Figure 1b). Within the respective San Juan NF, PDSI values were positive during both 2014 and 2019, indicating wetter than average years (Figure 1b, Table S1). See Kerr et al. (2022) for more information regarding climatic conditions for plots within the San Juan NF.

2.1 | Field sites

In 2014, 15 study plots were established in natural aspen stands in the San Juan NF of Southwest Colorado at the lower elevation

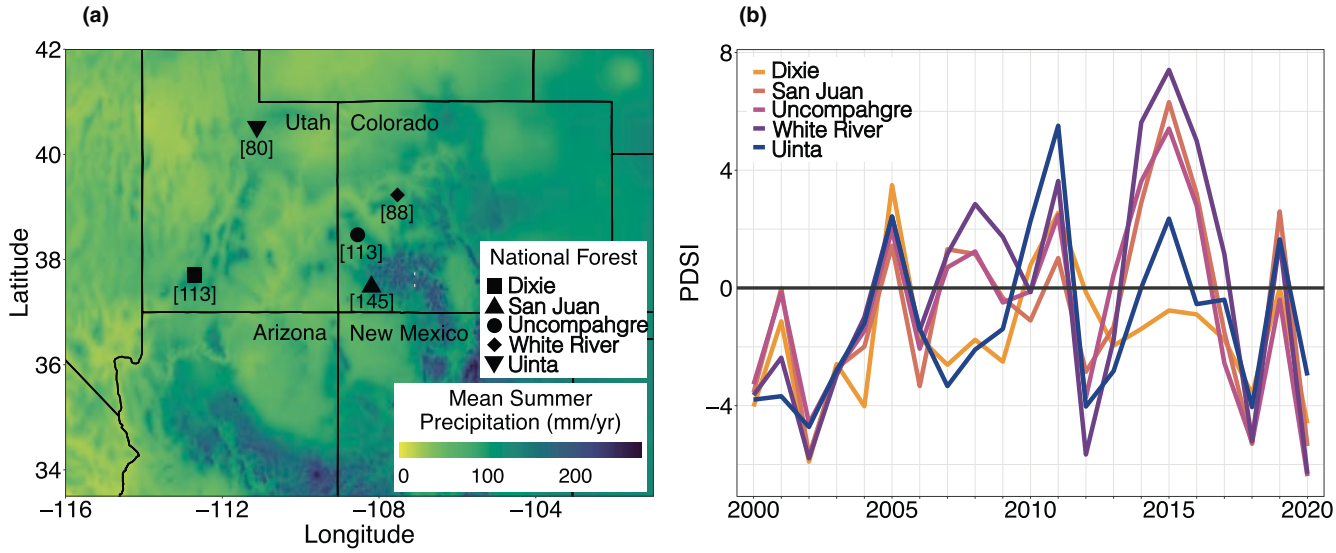

FIGURE 1 Summer precipitation and drought conditions for the southwestern United States. The North American Monsoon (NAM) pattern largely influences the states of Arizona and New Mexico, which receive the majority of their summer precipitation (July and August) from 1961 to 1990. The aspen populations used in this study are represented by points and occur in the Dixie, San Juan, Uncompahgre, White River and Uinta National Forests (NFs). Numbers in brackets indicate the mean summer precipitation, and mean values for each population are given in brackets underneath the points on the map. (b) Summer (July and August) Palmer Drought Severity Index (PDSI) values from 2000 to 2020 (TerraClimate, Abatzoglou et al., 2018) obtained from TerraClimate.

range margin (low, 2669 m), range centre (mid, 3108 m) and range margin (high, 3547 m) of interest that ranged in elevation. These plots were selected to maintain relatively consistent slopes and aspects to avoid microtopographic variation (Table S2). In 2018, an additional two and one plots were established at the lower and mid-range margins, respectively, to replace plots that had completely died off since 2014. In total, 15 plots were established in each of five natural aspen populations in the Dixie, San Juan, Uncompahgre, White River and Uinta NFs of Utah and Colorado (Figure 1; Table S2). These plots were selected from a candidate list of natural aspen populations that spanned a climate gradient from cool, wet to hot, dry climates that had been generated from the United States Forest Service Forest Inventory and Analysis database. The 2020 study plots were selected to have similar slopes, aspects and elevation, so that macroclimate differences were the main climate differences among the populations (see Table S2 for more detail on site conditions). All study plots were 18-m radius, circular plots and centre points were marked with a GPS unit (Trimble Geo 7x, Trimble Navigation Ltd.). Surveys of 2014, 2018, 2019 and 2020 were conducted to document the diameter at breast height (DBH) for every tree within each plot (DBH ranged from 11.4 to 21.5 cm across all plots; Table S2). Plots were revisited the following growing seasons (2019 for the San Juan elevation transect and 2021 for the multi-forest comparison) and trees were visually scored for health and recent canopy dieback (i.e. mortality). Because 2018 and 2020 were severe drought years for these populations, evaluating canopy dieback provides a useful estimate of how trait variation mediates drought-induced mortality among the natural populations studied here.

Geographic (i.e. latitude, longitude, elevation) and climatic variables of interest for each plot were extracted for the years 2014–2020 (TerraClimate, Abatzoglou et al., 2018): maximum temperature (Tmax, °C), precipitation accumulation as snow water equivalent (SWE, cm). PPT from 1961 to 1990 was used to determine precipitation that occurs as summer rainfall (July, August) in the absence of drought, as this period was targeted to provide historic estimates of summer rainfall prior to the intense and prolonged drought that the San Juan has experienced in recent decades. No permits were required for fieldwork in this study.

2.2 Measurements

Within each plot, healthy and mature individual trees (three trees in 2014, five in all other years) were selected for branch-level measurements of $A_L:A_S$. Plots were visited from late June to early July of 2014, 2018, 2019 and 2020, and one to three branch samples per focal tree were collected from sunlit, upper parts of the canopy using a pole pruner or shotgun within each plot. While leaf phenology was not tracked in this study, aspen in the region have been shown to start their growing season (Moser et al., 2015) with leaf full leaf development and new branch growth occurring during our measurement timeframes. The broken end of each branch was immediately wrapped in a wet paper towel, placed in a moist plastic bag and into a cooler for transport back to the laboratory.

Branch segments were cut under water using a sharp razor blade to produce branch samples with sapwood diameters ~5 mm

and lengths of ~10 cm to accommodate vessel length (Sperry et al., 1991). Hydraulic conductance on the samples was measured with the pressure-flow method (Sperry et al., 1988) with a 20 mM potassium chloride solution filtered to 0.2 μm. Native conductance (*k*nat) was measured, then samples underwent overnight vacuum infiltration to remove embolisms and determine maximum conductance (*k*max). Percent loss conductance (PLC), which represents the degree of native embolisms present in the sample (Equation 1), was quantified as

$$\mathrm{PLC}(\%) = \left(\frac{k\max - k\mathrm{nat}}{k\max}\right) \times 100. \quad (1)$$

Total sapwood-only leaf area was quantified using the cut branch as the distal to the cut branch as the proximal boundary (used to estimate canopy-level leaf area) in 2014, 2018, and a LI-3100C area meter (Li-Cor Biosciences) in 2019, 2020), and ImageJ (Schneider et al., 2012). Sapwood area was calculated from the diameter of the sapwood at the basal end of the branch segment, and ratios of A_L:A_S were calculated by dividing A_L by A_S. Previous work in the San Juan NF suggests aspen branches of this size retain ~8 years of growth on average, estimated the age of the branch sections in this study (Anderegg et al., 2013). For the San Juan NF, a baseline for A_L:A_S is assumed to be reflected in the 2014 results as this was an average climatic year for these plots. For all of the forests in 2020, the Uinta NF provides a baseline for A_L:A_S. This population is the least reliant on monsoonal summer precipitation and had the least negative PDSI value in 2020 (Figure 1b). Therefore, A_L:A_S values in the Uinta NF trees are likely to represent the least stressful combination of leaf demand versus supply.

We also investigated whether branch-level patterns scaled up to stand-level by analysing variation in both stand-level leaf area indexes (LAIe) versus sapwood area (SA) stand-level basal area indexes (BAI_8) given that branches typically retain ~8 years of growth (see above). ment core was collected at breast height from 15 focal trees from each of the study plots established in 2020 (n = 90 cores est). During collection, sapwood depth (cm) was recorded by marking the point where the sapwood transitions to heartwood. This point was determined by holding the core to the sun, as sapwood transmits more light than heartwood due primarily to differences in water content (Kaufmann & Troendle, 1981). In the laboratory, cores were mounted and sanded with progressively finer sandpaper until ring-width boundaries were visible under a microscope. Cross-dating was verified at the $p < 0.01$ significance and using a 50-window, which overlaps program COFECHA (Holmes, 1983). The 'dplr' (v.1.7.2) R package was used to convert raw ring widths to basal area increment (BAI; Bunn, 2008), and the total BAI of the forest (2013–2020 for the 2020 study plots, and 2011–2018 for the San Juan NF plots) was determined. SA was first calculated using the cores for each forest by Equation (2):

$$\mathrm{SA} = \pi\left((\mathrm{DBH}_i \times \mathrm{sd}_i) - (\mathrm{sd}_i)^2\right), \quad (2)$$

where sd_i is the ith tree's (sapwood depth and DBH_i is the ith tree's diameter at breast height. This equation shape. Although trees may not be perfectly circular, this is a standard assumption and is considered sufficiently accurate. SA was then estimated for all trees in each study plot using a power regression model fit between tree DBH and SA (Figure S1; Meinzer 2001). BAI_8 was also estimated for all trees in each study plot using linear regression models fit between tree DBH and BAI_8 (Figure S2).

We assessed whole stand leaf area using more direct observations of leaf area index (LAI). In 2000 an plant canopy analyser was used to measure LAI within the San Juan elevation transect plots according to methods in the manual with (Li-Cor Biosciences, 1992). Three sensor lens readings (used below the canopy (~1 m above ground) and moved to ferent spots within each plot (plot each cardinal direction) to capture variability within the plot canopy. In June/July 2020, hemispherical photos were used to measure LAI in all forest plots using Gap Light Analyser software (GLA v2; Frazer et al., 1999). Photographs were taken at 5 different spots within each plot (one in the centre and each at 10 m distance in each cardinal direction) to capture within plot canopy variability. We used the LAI 4-ring output variables which represent estimated LAI integrated over zenith angles of 0–60°. For 2000 to the analyses, photographs were taken at dawn or dusk to ensure direct overhead sun did not affect LAI estimates.

2.3 Statistics

Linear mixed models were constructed to measurement values (A_L:A_S, LAI:SA, LAI:BAI_8) among the populations in 2020 (Figure 2B,C,E), among the San Juan NF aspen for the most recent 8 years (Figure 2D,F), and across elevations and years in the San Juan NF from 2014 to 2020 (Figure 2B). Linear mixed models were also constructed to relate absolute measurement values of PLC among the 2020 populations. For the 2020 population analyses, we used the fixed effect of population. For the 2018 San Juan NF analyses, elevation and the random effect of plot. For the interannual San Juan NF analyses, we used the fixed effect interaction, and the random effect of tree to account for repeated measures. Model assumptions of normality were visually assessed with diagnostic plots of residuals. The effects of population, elevation, year and elevation-year interaction were determined with likelihood ratio tests (LRT) by comparing the full model with reduced models. When effects were significant, pairwise comparisons were made between groups using the estimated marginal means and the Tukey method for p-value adjustments.

Linear regressions were used to test for significant relationships between previous year SWE and current year July precipitation for all years from 1959 to 2020. The month of July is typically when summer monsoon rainfall occurs in this region. To determine if mortality in natural populations was

mediated by variation in A_L:A_S and LAI:SA, linear regressions were also used to test for significant relationships between leaf area: sapwood area (A_L:A_S, LAI:SA), July precipitation during the year of the drought, and % canopy dieback scored in 2019 or 2021 (the years following each drought). Plot-level values for A_L:A_S were averaged, resulting in a single data point per forest. Coefficients of determination (R^2) and *p*-values were determined through linear regressions.

Computational and statistical analyses were conducted in R version 4.2.1 (R Core Team, 2021). The 'lme4' (version 1.1.30), 'lmerTest' (version 3.1.3), and 'emmeans' (version 1.8.3) packages were used to construct and fit mixed-effects models (Bates et al., 2015; Kuznetsova et al., 2017; Lenth, 2022). Significance of fixed effects was determined with Satterthwaite approximation methods conducted using 'emmeans'. The 'car' package (version 3.1.0) was used to plot QQ normal lines with 95% confidence intervals for linear model assumptions (Fox et al., 2018). For all analyses, significance levels of <0.05 and =0.05–0.1 were considered statistically significant and marginally significant, respectively.

3 | RESULTS

3.1 | Variation in A_L:A_S across temporal and climatic gradients

For branch-level patterns, aspen populations in southern latitude forests and at low elevations within the San Juan NF generally allocated significantly more leaf area per unit of sapwood area (i.e. higher branch-level A_L:A_S) during the 2018 and 2020 severe drought years (Figure 2A,B) compared to assumed baselines (2014 values for the San Juan NF and the Uinta NF values for 2020; see methods for more detail on the determination of baselines).

For stand-level patterns, aspen populations (Figure 2C) and at low elevations with the San Juan NF (Figure 2D) also allocated significantly more leaf area per unit of sapwood area (i.e. higher stand-level LAI:SA) during the 2018 and 2020 severe drought years. In addition, aspen populations in the Dixie NF (Figure S1), which seems to drive the differences for this population between branch- and stand-level patterns of leaf area ratios (e.g. Figure 2A vs. C). Patterns in leaf area (LAI) corroborated higher leaf area within the San Juan NF during both the 2018 and 2020 droughts (Figure 2E,F). While LAI was not significantly higher in low elevation aspen in the San Juan NF during 2018, it is notable that low elevation aspen which experienced the most dieback (Figure 2F). Contrary to LAI:SA patterns, LAI was generally reduced in lower latitude, more monsoonal aspen populations, apart from the San Juan NF (Figure 2E). The low and mid elevation aspen in the San Juan NF had many recently dead aspen trees, which suggests that LAI prior to die-off may have been closer to the more northern forests.

3.2 | NAM and leaf production patterns in monsoon-dependent populations of aspen

Using a 62-year dataset of gridded climate variables for each forest/elevation band, we quantified the snow water equivalent (SWE) and July precipitation years were linked with stronger monsoonal (July) rainfall in some of the locations where we documented structural overshoots. We observed negative relationships between SWE and increased summer precipitation in nearly all populations, and this relationship was marginally statistically significant for the San Juan NF ($R^2 = 0.060$, $p = 0.052$; Figure 3a). In contrast, we observed a statistically significant positive relationship between SWE and summer precipitation in the Uinta NF ($R^2 = 0.10$, $p = 0.01$; Figure 3a), the most northern latitude population that is least reliant on monsoonal rainfall. In the San Juan NF, there were consistent negative relationships whereby years with reduced SWE the preceding winter had higher summer NF precipitation (Figure 3b). This relationship was marginally statistically significant for the low ($R^2 = 0.050$, $p = 0.071$) elevation aspen population (Figure 3b).

Within the region of interest for this study, there have been several severe droughts in recent decades, including during the years of had significantly higher ratios of LAI:BAI_8 (Figure S3), suggesting that sapwood growth was likely slower than leaf area production in this population. Values of sapwood area were

FIGURE 2 Ratios of leaf area to sapwood area (A_L:A_S), leaf area to sapwood area ratios (LAI:SA) higher in aspen populations more reliant on summer monsoonal precipitation during the drought years of 2018 and 2020 and indicated possible structural overshoot. (A) Branch-level A_L:A_S among aspen populations from all National Forests (NF) in 2020. (B) Branch-level A_L:A_S among aspen populations within the San Juan NF during 2014, 2018, 2019, and 2020. (C) Stand-level LAI:SA among aspen populations from all NFs in 2020. (D) Stand-level LAI:SA among aspen populations within the San Juan NF during 2018. (E) LAI among aspen populations from all NFs in 2020. (F) LAI among aspen populations within the San Juan NF during 2018. In (A), (C) and (E), aspen populations have been arranged according to the amount of summer monsoonal precipitation they receive (high to low). Significant differences between forests are indicated by unique lowercase letters. In (B), (D) and (F), aspen gradient they occur along (lower elevation, more monsoonal precipitation, orange to higher elevation, less monsoonal precipitation, blue). In (B), significant within a single elevation zone are indicated by colour-matching lowercase letters, while the asterisk indicates that only within 2018 low-elevation aspen had significantly higher branch-level A_L:A_S compared to mid- and high-elevation aspen. In (D) and (F), significant differences between sites are indicated by unique lowercase letters. In (A) and (B), median branch-level A_L:A_S (center bar), interquartile range (IQR, boxes), and outlying points (points). In (C)–(F), bars represent means and error bars represent 95% confidence intervals.

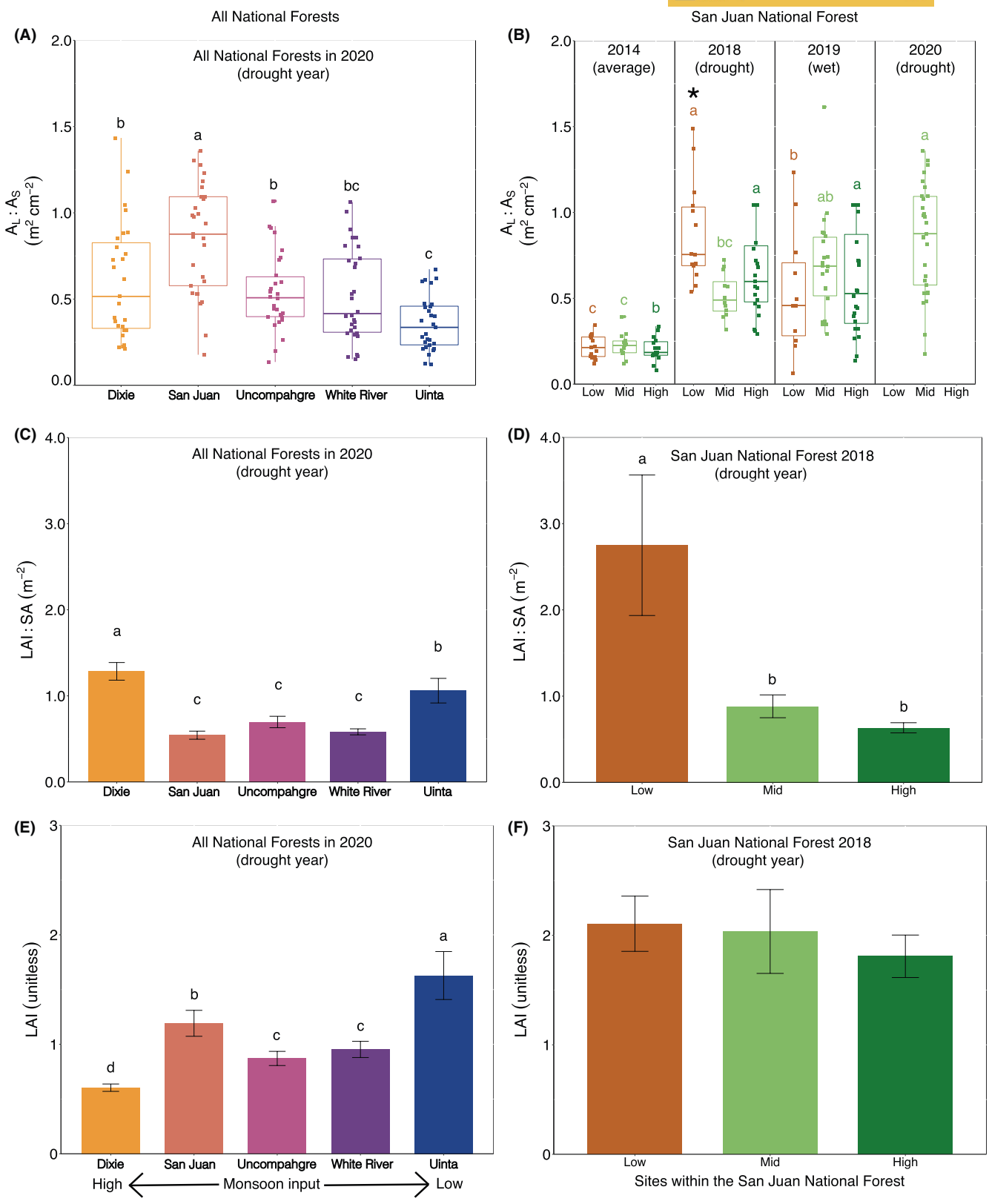

2002, 2018 and 2020 (Williams et al., 2020). In general, these drought years failed to materialize and bring substantial rainfall to the forests during the San Juan NF; Figure 3, Table S1), which may have contributed to drought-driven aspen mortality in the region of our investigation.

3.3 | Maladaptive leaf area shrinkage overshoot and increased mortality

2018 in the Dixie NF and 2020 in During 2020, trees from more southern latitude populations (Dixie, San Juan and Uncompahgre)

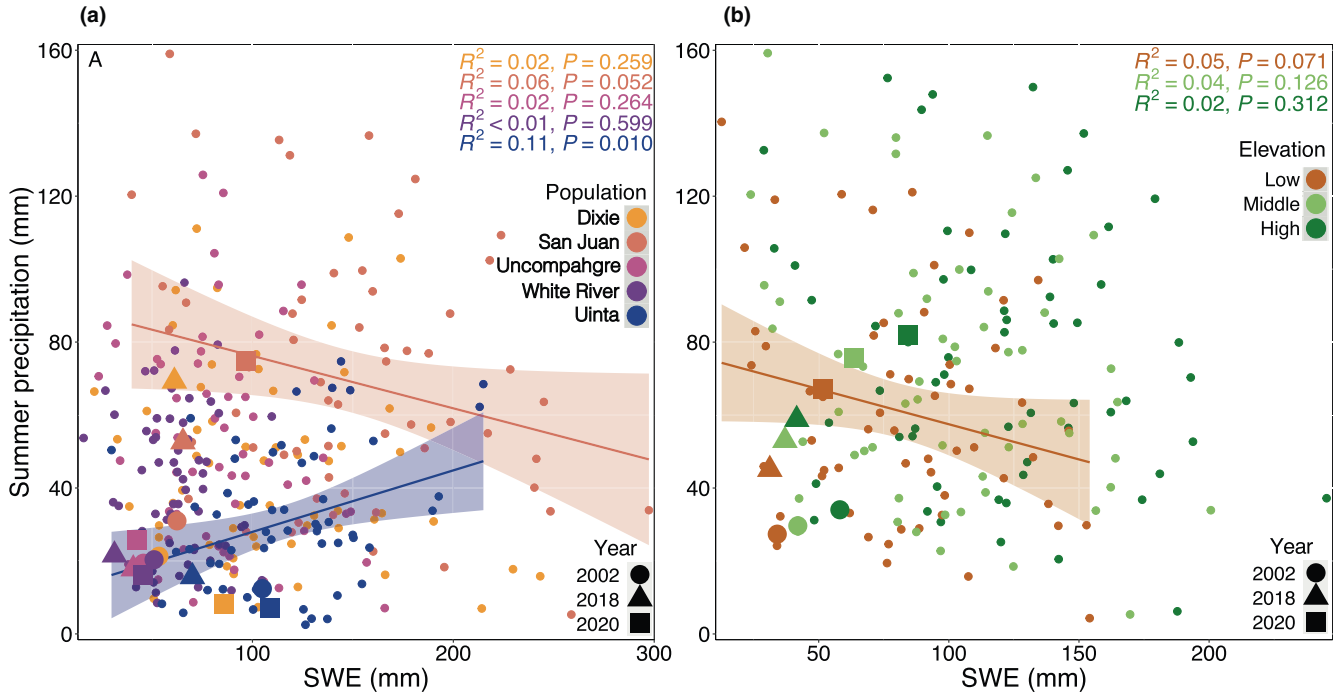

FIGURE 3 Low snowpack years are linked with stronger monsoonal rainfall. Relationships between snow water equivalent (SWE, November–March) and mean summer (July) precipitation at (a) the high elevation site within the Uncompahgre NF and (b) the low elevation site within the San Juan NF. Points represent annual values for each population/elevation band between 1958 and 2020. Larger points that vary by shape indicate severe drought years (2002, 2018, 2020). Lines represent linear model regression fits (R^2 and p-values from linear models assessing significance of SWE as a predictor of summer precipitation; significant at $p < 0.05$) for each population/elevation site. Shaded regions represent 95% confidence intervals and are also coloured according to population/elevation band.

loss of branch hydraulic conductance, indicating potentially heightened drought stress, albeit these results were not statistically significant (Figure S4). Structural overshoot was partially associated with increased mortality risk following severe drought across populations and sites. At the branch level, populations with more leaf production or lower sapwood production (i.e. higher branch-level $A_L:A_S$) during the 2018 and 2020 drought years had more canopy dieback the following growing season ($R^2 = 0.53$, $p = 0.02$; Figure 4a), a relationship particularly notable for populations from southern latitudes within the San Juan NF. Similarly, populations with higher stand-level LAI:SA during the 2018 and 2020 drought years also had more canopy dieback the following growing season, albeit this relationship was not statistically significant ($R^2 = 0.32$, $p = 0.243$), and seems to be driven primarily by the low elevation zone of the San Juan NF (Figure 4b). Neither LAI:SA during the drought year, July precipitation during the drought year (PPT), nor their interaction term had significant effects on canopy dieback the year following drought (Figure 4b).

4 | DISCUSSION

In this study, we quantified leaf area–sapwood area relationships and drought-induced mortality across natural populations of aspen within National Forests (NF) that span the northern transition zone of the North American Monsoon. Variation in $A_L:A_S$ was correlated with tree canopy dieback following drought and highlighted the potential as an underlying mechanism for aspen leaf production in this region. These results support the hypothesis that too much biomass was allocated to tree leaf area per unit sapwood area, resulting in structural overshoots that were not supported by sufficient soil moisture during severe drought periods. Observed increases in canopy dieback following severe drought years suggest that this maladaptive trait plasticity led to increased hydraulic stress and aspen mortality.

4.1 | Variation in $A_L:A_S$ across temporal and spatial gradients

In general, ratios of leaf area to sapwood area were observed to be higher among aspen populations in warmer, drier regions that are more reliant on NAM summer precipitation, a pattern consistent with the hypothesis of structural overshoot at both the branch and stand level. Given that sapwood area in aspen is determined by multiple years' worth of growth (8 or more years in the size of the branches we measured which may be potentially more than in tree trunks), this overshoot is likely driven by a mismatch between leaves given

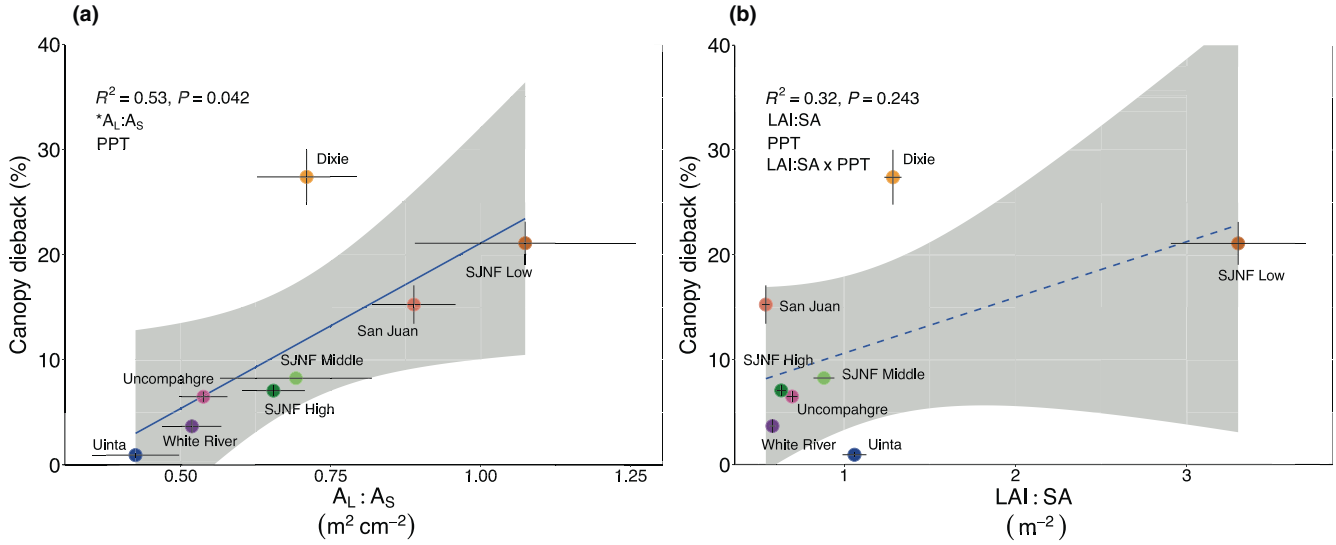

FIGURE 4 Aspen populations with higher leaf area to sapwood area (A_L:A_S) had greater canopy dieback the following season. (b) This relationship was also found for stand-level leaf area index (LAI) and leaf area to sapwood area (LAI:SA). Points represent mean values and error bars represent standard errors (in some cases, error bars are smaller than the point). Data are from 12 aspen stands in the Dixie, Fishlake, Manti-La Sal, San Juan, Uinta-Wasatch-Cache, and White River National Forests (NF) during 2020, and elevation ranged from 2,400 to 3,200 m (with the lowest elevation stands at the warm and dry margins in the San Juan NF during 2018). Blue lines represent linear model regression fits (the R^2 and p values from the models are printed on the figures and solid lines indicate a significant relationship), and shaded regions represent 95% confidence intervals. Summaries from the linear regression models are printed on the figures (A_L:A_S or LAI:SA) and July 1 to June 30 precipitation during the drought year (PPT). Asterisks indicate statistically significant differences from the model where * is $p < 0.05$.

architecture. This could be further explored in understanding the response of stand-level ecosystem function and radial growth after leaf area is already set. However, results between branch-level A_L:A_S and stand-level LAI:SA were not identical, which indicates there are disconnects between branch- and stand-level leaf allometry patterns that remain to be resolved. A_L:A_S typically declines with tree age (Mencuccini et al., 2005), and the two monodominant populations with the highest LAI:SA (Dixie and San Juan National Forest) were notably shorter than the other populations. Moreover, there is likely variation in A_L:A_S with tree size across these populations, which combines with variation in the stand size-distribution to complicate the branch-to-stand scaling. As a result, sapwood areas were much smaller for trees in the Dixie NF compared to the other populations, which may be particularly prevalent in drought-prone regions that do not have time to recover between large differences between branch- and stand-level ratios of leaf area production. In addition, canopy structure (e.g. branch orientation, number of branches, canopy height, etc.) in these aspen stands may differ due to differences in site geography (Zhang et al., 2016) or due to seasonal variability (Wirth et al., 2001), representing another form of plasticity that might mediate forest mortality. Importantly, our data only reflect leaf area to sapwood area ratios for a single time point, and dynamics involving seasonal variation in these ratios might alter the findings reported here.

Notably, the LAI and LAI:SA results suggest that stand-level changes like large-scale tree die-offs counteract the tissue-scale A_L:A_S overallocation of individual trees. Branch-level A_L:A_S provides a solid metric for 'physiological acclimation' (i.e. acclimation at the tissue level) but not a strong metric for 'ecosystem acclimation' (i.e. acclimation at the stand level). This latter metric is important for understanding the response of stand-level ecosystem function and for modelling aspen forest response to future climate change (Sperry et al., 2019), making the disconnect between branch and stand-level allometry a critical problem to solve. These results may also be indicative of a stand-level compensating mechanism, whereby aspen trees with more canopy dieback have fewer branches but higher leaf area per branch (Doi, 2022), which may be particularly prevalent in Sa
disturbance (Doi et al., 2008). However, we did observe elevated percent loss of hydraulic conductance in trees during the 2020 drought, especially among populations with the lowest summer precipitation (Figure S4), but this cannot completely confirm that canopy dieback occurred from hydraulic failure due to increased evaporative demand from more leaf production. Scaling estimates of water transport from the level of tissue to the level of whole tree or plot also remains a challenge for modelling aspen forest response to climate change (Meinzer et al., 2005; Mencuccini et al., 2019).

4.2 | NAM and leaf production p
monsodoenp-endent populations of

Higher branch-level A_L:A_S and stand-level LAI:SA during the severe drought years observed in this study, and at lower, drier elevations, may put aspen trees at increased risk for physiological stress and damage, given increased evaporative demand and therefore seem to indicate a structural overshoot (Jump et al., 2017). Production of leaf area may have been influenced by other environmental signals prior

to growing-season drought development, such as autumnal climatic conditions during vegetative bud set in the previous growing season or warmer spring temperatures that resulted in advanced phenology during 2018 and 2020 (Gordo & Sanz, 2010; Uemura et al., 2000). Given that low snowpack years have been historically correlated with stronger monsoonal rainfall through potential land-atmosphere feedbacks (Notaro & Zarrin, 2011; Zhu et al., 2005), increased leaf area in southern latitude aspen populations may also be the result of some combination of genetic differences and/or advanced phenology in response to earlier snow melt-off and warmer spring temperatures in anticipation of heavier summer monsoon rainfall.

The overall low coefficients of variation in our climate analyses (Figure 3) indicate that monsoon variability is influenced by many factors in addition to preceding winter snowpack. However, the negative relationships seen here between snowpack and summer precipitation in monsoon-dependent forests are consistent with documented land-atmosphere feedback mechanisms in both observational datasets and climate models (Gutzler & Preston, 1997; Notaro & Zarrin, 2011; Zhu et al., 2005). Yet low snowpack is only one possible mechanism influencing the NAM, and further investigations into other climatic drivers will be important for better understanding aspen forest responses to future climate change in NAM-dependent ecosystems. Predicting where mismatches in leaf production and NAM precipitation may occur between leaf production and substantial canopy dieback, tending to severe drought years in this study, may provide better insight into which forest stands are most at risk of drought-induced mortality.

It is important to note that water uptake by aspen may be further complicated by the fact that this is a clonal species where individual trees (ramets) are connected to neighbouring ramets through a shared root system (Barnes, 1966; Mitton & Grant, 1996). Previous work suggests that resources are likely shared between ramets via the root system (Baret & DesRochers, 2011; De Byle, 1964), yet studies focused on water limitation and mortality patterns in aspen and balsam poplar (*Populus balsamifera*) indicate ramets can act more like individual trees (i.e. little evidence of facilitation and resource sharing) under drought (Adonsou et al., 2016; Anderegg et al., 2012). The 'pipe model theory' which states that water transport capacity in the stems determines canopy leaf area (Shinozaki et al., 1964), may not apply as simply for a clonal species like aspen although work has shown that naturally occurring aspen ramets in the Sierra Nevada of California do conform to this theory (Caldwell & O'Hara, 2017). It remains unknown how much clonal rooting dynamics influence biomass allocation patterns within the entirety of a clone or across the distribution of aspen forests.

4.3 | Leaf area structural overshoot and drought-induced mortality risk

While tree mortality can arise due to several abiotic and biotic factors, aspen mortality following drought has been strongly linked to hydraulic failure and the loss of water-conducting tissue within the xylem of the trees (Anderegg et al., 2012), particularly driven by the drying of shallow soils during the mid/late growing season (Anderegg et al., 2013; Bell et al., 2014; Refsland & Cushman, 2021). Therefore, the low precipitation during the critical drought years of our study (2018 and 2020), combined with elevated spring and summer temperatures, may have resulted in a lack of water supply to meet the evaporative demand of more leaf area and was likely important in driving spatial patterns of aspen mortality as seen in the significant positive relationship between branch-level A_L:A_S and canopy mortality. While the stand-level LAI:SA relationship with canopy mortality showed the same trend as branch-level A_L:A_S, we hypothesize the non-significant relationship with LAI:SA may be related to higher variation and uncertainty in scaling relationships from branch to stand. Current climate change scenarios predict more frequent drought events for this region, which could be particularly lethal if the seasonal couplings between snowpack and summer precipitation become more decoupled (Pascale et al., 2017; Seager et al., 2007).

The canopy dieback results reported here may not be indicative of complete tree mortality, yet aspen in this region has been shown to exhibit a high degree of drought tolerance in mesic forests, and structural overshoot during the 2018 and 2020 droughts will likely continue to unfold over the next decade through mortality of canopy dieback tends to proceed to full mortality within 6–10 years (Anderegg et al., 2013; Worrall et al., 2010). A structural overshoot may be an important mechanism as mortality often lags multiple years after the initial inciting drought (Anderegg et al., 2013; Trugman et al., 2018).

Importantly, we were unable to test for the effects of biotic mortality agents on canopy dieback in this study. While an ultimate cause of mortality may be pathogenic or biotic, drought stress can decrease the capacity for aspen trees to fight off pests and pathogens, which can be a significant contributor to mortality, especially in the drought-prone regions of the southwestern United States (Marchetti et al., 2011). Aspen trees in this study, particularly in regions more reliant on NAM precipitation, showed substantial loss of hydraulic conductance during the 2020 drought (Figure S4), indicative of some drought-related stress.

Our results suggest that variation in A_L:A_S is associated with aspen tree drought response, which highlights the importance of understanding the underlying mechanisms of leaf phenology and leaf production and their implications in mass allocation and climate forecasting. The environmental signals involved in leaf phenology and leaf development are complex and may be due to a combination of both current year and previous year climate (Gordo & Sanz, 2010; Uemura et al., 2000). Inclusion of soil moisture parameters, such as snow moisture, in addition to the traditional parameters used in most phenological models (i.e. growing degree days) may allow for improved model predictions (Richardson et al., 2013). Determining the direct climate signals involved in leaf area production and their timing may also improve our ability to model biomass and resource allocation in aspen forests under a changing climate

(Rosas et al., 2019). Among our aspen populations, we observed substantial intraspecific variation in A_L:A_S, which occurred across both spatial and temporal scales. Incorporating intraspecific trait variation into trait-based models that account for important functional traits like A_L:A_S will be crucial for improving our ability to forecast forest response to future climates (Anderegg, 2015; Sabot et al., 2022; Xu et al., 2021).

The findings reported here have broader implications for other tree species and forested ecosystems. Across other species types, there is substantial evidence that ratios of leaf area to sapwood area conform to evolutionary theory, highlighting the potential impact of this trait on fitness. For instance, A_L:A_S typically increases with increasing aridity (i.e. less leaf area production in warmer/drier conditions; Zhu & Zhao, 2023), decreased A_L:A_S with lower stem hydraulic conductance (i.e. lower leaf area to match water conductance capacity; Magnani et al., 2000), and declining A_L:A_S with increasing tree height (i.e. maintenance of leaf-specific hydraulic efficiency with constrained whole-plant hydraulic conductance; McDowell et al., 2002). However, there are also deviations from these findings which suggest ratios of leaf area to sapwood area may not be as tightly linked to climate and environmental signals in all cases. Zhu and Zhao (2023) also found significant interaction effects between temperature and precipitation that resulted in opposite trends in A_L:A_S, indicating complex responses to environmental signals. Other studies have found no relationship between A_L:A_S and tree height (Mencuccini et al., 2019; Meinzer et al., 2005) or reported increasing A_L:A_S with tree height for two species (*Picea abies* and *Abies balsamea*), the advantages to which appear to be unclear (Coble et al., 2018). Similarly, Bradford et al. (2008) found no shifts in A_L:A_S among *Pinus edulis* and *Juniperus monosperma* trees after a 5-year warming and drought experiment. Acclimation processes involving leaf area to sapwood area ratios can take longer than one stressful growing season. Thus, further elucidating and disentangling the drivers of leaf area to sapwood area ratios in the future would provide valuable insight into understanding how this key trait informs modelling and projections of future forest ecosystem dynamics.

5 | CONCLUSIONS

Our study connects leaf area overshoot patterns to elevated mortality in a widespread tree species. These results provide an example of likely maladaptive trait plasticity that led to increased stress and mortality during severe droughts. They highlight that trait-environment relationships are often complicated and may be due to trait responses to complex or differing climate cues and that plant allocation responses during stress are a major research need (De Kauwe et al., 2014; Falster et al., 2015). When and where trait plasticity is adaptive, leading to increased climate resilience versus maladaptive, leading to increased tree mortality, as well as consideration of how stand-level acclimation through changes in density affects mortality over long timescales, remain key questions for illuminating the future of forests in the 21st century.

AUTHOR CONTRIBUTIONS

The study was designed by Kelly L. Kerr, Leander D. L. Anderegg, Anna T. Trugman and William R. L. Anderegg. Data collection and analyses were carried out by Kelly L. Kerr and Leander D. L. Anderegg, while data interpretation was carried out by Kelly L. Kerr, Leander D. L. Anderegg, Anna T. Trugman and William R. L. Anderegg. Kelly L. Kerr led the writing of the manuscript, and Kelly L. Kerr, Leander D. L. Anderegg, Anna T. Trugman and William R. L. Anderegg contributed to drafts and gave final approval for publication.

ACKNOWLEDGEMENTS

The authors thank Jayce Cappiert, Shelby Jenkins, Caleb Kastelic, Elizabeth Schattle, Sophie Buyesse and Grayson Badgley for their assistance with field and laboratory work. K.L.K. acknowledges support from the University of Utah Global Change and Sustainability Center and the University of Utah Graduate Research Fellowship. L.D.L.A. and A.T.T. acknowledge support from US National Science Foundation grants (NSF 2003205; 2216855). L.D.L.A. acknowledges support from USDA Agriculture and Food Research Initiative 1027700. A.T.T. acknowledges support from the Gordon and Betty Moore Foundation Grant GBMF119-74. W. support from the David and Lucille Packard Foundation, the Blavatnik Family Foundation, the US National Science Foundation grants IOS-1802880, 2003017, 2044937, and the Alan T. Waterman Award IOS-2325700.

CONFLICT OF INTEREST STATEMENT

The authors declare no conflicts of interest.

DATA AVAILABILITY STATEMENT

Data deposited in the Dryad Digital Repository: http://doi.org/10.5061/dryad.d83q3 (Kerr et al., 2025).

ORCID

Kelly L. Kerr https://orcid.org/0000-0002-0830-2148

REFERENCES

Abatzoglou, J. T., Dobrowski, S. Z., Parks, S. A., & Hegewisch, K. C. (2018). TerraClimate, a high-resolution global dataset of monthly climate and climatic water balance from 1958-2015. *Scientific Data*, *5*, 1–12.

Adams, D. K., & Comrie, A. C. (1997). The North American monsoon. *Bulletin of the American Meteorological Society*, *78*, 2197–2213.

Adonsou, K. E., DesRochers, A., & Tremblay, F. (2016). Physiological integration of connected balsam poplar ramets. *Tree Physiology*, *36*, 797–806.

Anderegg, L. D. L., Anderegg, W. R. L., & Berry, J. A. (2013). Drought characteristics' role in widespread aspen forest mortality across Colorado, USA. *Global Change Biology*, *19*, 1526–1537.

Anderegg, W. R. L., Anderegg, L. D. L., & Huang, C. (2019). Testing early warning metrics for drought-induced tree physiological stress and mortality. *Global Change Biology*, *25*(7), 2459–2469. https://doi.org/10.1111/gcb.14655

Anderegg, L. D. L., Loy, X., Markham, J. H., Ellsworth, D. S., & Anderegg, W. R. L. (2015). Hierarchical tree and leaf water traits and sensitivity to water deficit: Elevated CO2 effects on poplar physiology and leaf traits do not increase drought tolerance. *Tree Physiology*, *35*, 1310–1320.

Anderegg, W. R. L., Anderegg, L. D. L., Kerr, K. L., & Trugman, A. T. (2019). Widespread drought-induced tree mortality at dry range edges indicates that climate stress exceeds species' compensating mechanisms. *Global Change Biology*, *25*, 3793–3802.

Anderegg, W. R. L., Flint, A., Huang, C., Flint, L., Berry, J. A., Davis, F. W., … Field, C. (2015). Tree mortality predicted from drought-induced vascular damage. *Nature Geoscience*, *8*, 367–371.

Anderegg, W. R. L., Hicke, J. A., Fisher, R. A., Allen, C. D., Aukema, J., Bentz, B., … Macalady, A. (2015). Tree mortality from drought, insects, and their interactions in a changing climate. *New Phytologist*, *208*, 674–683.

Anderegg, W. R. L., Trugman, A. T., Bowling, D. R., Salvucci, G., & Tuttle, S. E. (2019). Plant functional traits and climate influence drought intensification and land–atmosphere feedbacks. *Proceedings of the National Academy of Sciences of the United States of America*, *116*, 14071–14076.

Bradford, J. B., Schlaepfer, D. R., Lauenroth, W. K., & Burke, I. C. (2008). Shifts in plant functional type cover and aboveground production in response to an altered soil resource mosaic. *Ecosystems*, *11*, 1–16.

Brodribb, T. J., Bowman, D. J. M. S., Nichols, S., Delzon, S., & Burlett, R. (2010). Xylem function and growth rate interact to determine recovery rates after exposure to extreme water deficit. *New Phytologist*, *188*, 533–542.

Brodribb, T. J., Powers, J., Cochard, H., & Choat, B. (2020). Hanging by a thread? Forests and drought. *Science*, *368*, 261–266.

Coble, A. P., Cavaleri, M. A., Hofmeister, K. L., Fischer, M. L., Burton, J. I., & Cook, R. L. (2018). Increasing aboveground carbon allocation after canopy loss in a mature deciduous forest. *Ecosystems*, *21*, 1485–1498.

Cochard, H., Barigah, S. T., Kleinhentz, M., & Eshel, A. (2008). Is xylem cavitation resistance a relevant criterion for screening drought resistance among *Prunus* species (Rosaceae)? *Journal of Plant Hydraulics*, *2*, 1–8.

Cochard, H., Damour, G., Bodet, C., Tharwat, I., Poirier, M., & Améglio, T. (2005). Evaluation of a new dynamic model to simulate the water relations of walnut trees. *Journal of Plant Hydraulics*, *1*, 1–8.

Cochard, H., Ewers, F. W., & Tyree, M. T. (1994). Water relations of a tropical vine-like bamboo (*Rhipidocladum racemiflorum*). *Journal of Experimental Botany*, *45*, 1085–1089.

Cochard, H., Peiffer, M., Le Gall, K., & Granier, A. (1997). Developmental control of xylem hydraulic resistances and vulnerability to embolism in *Juglans regia* L. during early growth. *Tree Physiology*, *17*, 705–710.

Cochard, H., Venisse, J.-S., Barigah, S. T., Brunel, N., Herbette, S., Guilliot, A., … Sotta, B. (2007). Putative role of aquaporins in variable hydraulic conductance of leaves in response to light. *Plant Physiology*, *143*, 122–133.

Cochard, H., Venisse, J.-S., Barigah, S. T., Kleinhentz, M., & Eshel, A. (2008). Is xylem cavitation resistance a relevant criterion for screening drought resistance among *Prunus* species (Rosaceae)? *Journal of Plant Hydraulics*, *2*, 1–8.

Cochard, H., Damour, G., Bodet, C., Tharwat, I., Poirier, M., & Améglio, T. (2005). Evaluation of a new dynamic model to simulate the water relations of walnut trees. *Journal of Plant Hydraulics*, *1*, 1–8.

Cochard, H., Ewers, F. W., & Tyree, M. T. (1994). Water relations of a tropical vine-like bamboo (*Rhipidocladum racemiflorum*). *Journal of Experimental Botany*, *45*, 1085–1089.

Cochard, H., Peiffer, M., Le Gall, K., & Granier, A. (1997). Developmental control of xylem hydraulic resistances and vulnerability to embolism in *Juglans regia* L. during early growth. *Tree Physiology*, *17*, 705–710.

Cochard, H., Venisse, J.-S., Barigah, S. T., Brunel, N., Herbette, S., Guilliot, A., … Sotta, B. (2007). Putative role of aquaporins in variable hydraulic conductance of leaves in response to light. *Plant Physiology*, *143*, 122–133.

geographic range of eight Australian trees. *New Phytologist*, *229*, 1375–1387.

Anderegg, W. R. L., Berry, J. A., Smith, D. D., Sperry, J. S., Anderegg, L. D. L., & Field, C. B. (2012). The roles of hydraulic and carbon stress in a widespread climate-induced forest die-off. *Proceedings of the National Academy of Sciences of the United States of America*, *109*, 233–237.

Ashfaq, M., Ghosh, S., Kao, S., Bowling, L. C., Mote, P., Touma, D., Rauscher, S. A., & Diffenbaugh, N. S. (2013). Near-term accerlation of hydroclimatic change in the western U.S. *Journal of Geophysical Research: Atmospheres*, *118*, 10676–10693.

Baret, M., & DesRochers, A. (2011). Physiological responses to defoliation in nondefoliated aspen suckers. *Botany*, *89*, 753–761.

Barnes, B. V. (1966). The clonal growth habit of American aspens. *Ecology*, *47*, 439–447.

Bates, D., Machler, M., Bolker, B., & Walker, S. (2015). Fitting linear mixed-effects models using lme4. *Journal of Statistical Software*, *67*(1), 1–48. https://doi.org/10.18637/jss.v067.i01

Bell, D. M., Bradford, J. B., & Lauenroth, W. K. (2014). Forest stand structure, productivity, and age mediate climatic effects on aspen decline. *Ecology*, *95*(8), 2040–2046. https://doi.org/10.1890/14-0093.1

Bunn, A. G. (2008). A dendrochronology program library in R (dplr). *Dendrochronologia*, *26*, 115–124.

Caldwell, B. T., & O'Hara, K. L. (2017). Crown-level leaf area index and root biomass in *Populus tremnuloides Michx*. supports the pipe model theory. *Journal of Biodiversity Management & Forestry*, *6*(4), 1–9.

De Byle, N. V. (1964). Detection of functional intraclonal aspen root connections by tracers and excavation. *Forest Science*, *10*, 386–396.

De Kauwe, M. G., Medlyn, B. E., Zaehle, S., Walker, A. P., Dietze, M. C., Wang, Y., Luo, Y., Jain, A. K., El-Masri, B., Hickler, T., Wårlind, D., Weng, E., Parton, W. J., Thornton, P. E., Wang, S., Colin Prentice, I., Asao, S., Smith, B., McCarthy, H. R., … Norby, R. J. (2014). Where does the carbon go? A model-data intercomparison of vegetation carbon allocation and turnover processes at two temperate forest free-air CO_2 enrichment sites. *New Phytologist*, *203*, 883–899.

DeLucia, E. H., Maherali, H., & Carey, E. V. (2000). Climate-driven changes in biomass allocation in pines. *Global Change Biology*, *6*(5), 587–593. https://doi.org/10.1046/j.1365-2486.2000.00338.x

Eagleson, P. S. (1982). Ecological optimality in water-limited natural soil-vegetation systems: 1. Theory and hypothesis. *Water Resources Research*, *18*(2), 325–340. https://doi.org/10.1029/wr018i002p00325

Falster, D. S., Duursma, R. A., Ishihara, M. I., Barneche, D. R., FitzJohn, R. G., Varhammar, A., Aiba, M., Ando, M., Anten, N., Aspinwall, M. J., Baltzer, J. L., Baraloto, C., Battaglia, M., Battles, J. J., Bond-Lamberty, B., van Breugel, M., Camac, J., Claveau, Y., … York, R. A. (2015). BAAD: A biomass and Allometry database for woody plants. *Ecology*, *96*, 1445. https://doi.org/10.1890/14-1889.1

Fox, J., Weisberg, S., Adler, D., Bates, D., Baud-Bovy, G., Ellison, S., Firth, D., Friendly, M., Gorjanc, G., Graves, S., Heiberger, R., Laboissiere, R., Monette, G., Murdoch, D., Nilsson, H., Ogle, D., Ripley, B., & Venables, W. (2018). *Package 'car': Companion to applied regression*. CRAN Repository.

Frazer, G. W., Canham, C. D., & Lertzman, K. P. (1999). *Gap Light Analyzer (GLA): Imaging software to extract canopy structure and gap light transmission indicies from true-color fisheye photographs, users manual and program documentation*. Simon Fraser University, and the Insitute of Ecosystem Studies.

Gleason, S. M., Butler, D. W., & Waryszak, P. (2013). Shifts in leaf and stem hydraulic traits across aridity gradients in eastern Australia. *International Journal of Plant Sciences*, *174*, 1292–1301.

Gordo, O., & Sanz, J. J. (2010). Impact of climate change on plant phenology in Mediterranean ecosystems. *Global Change Biology*, *16*, 1082–1106.

Greenwood, S., Ruiz-Benito, P., Martínez-Vilalta, J., Lloret, F., Kitzberger, T., Allen, C. D., Fensham, R., Laughlin, D. C., Kattge, J., Bönisch, G., Kraft, N. J., & Jump, A. S. (2017). Tree mortality across biomes is promoted by drought intensity, lower wood density and higher specific leaf area. *Ecology Letters*, *20*(4), 539–553. https://doi.org/10.1111/ele.12748

Gutzler, D. S., & Preston, J. W. (1997). Evidence for a relationship between spring snow cover in North America and summer rainfall in New Mexico. *Geophysical Research Letters*, *24*, 2207–2210.

Holmes, R. L. (1983). *Program COFECHA user's manual*. Laboratory of Tree-Ring Research, University of Arizona.

Jump, A. S., Ruiz-Benito, P., Greenwood, S., Allen, C. D., Kitzberger, T., Fensham, R., Martínez-Vilalta, J., & Lloret, F. (2017). Structural overshoot of tree growth with climate variability and the global spectrum of drought-induced forest dieback. *Global Change Biology*, *23*(9), 3742–3757. https://doi.org/10.1111/gcb.13636

Kaufmann, M. R., & Troendle, C. A. (1981). The relationship of leaf area and foliage biomass to sapwood conducting area in four subalpine Forest tree species. *Forest Science*, *27*, 477–482.

Kerr, K. L., Anderegg, L. D. L., Trugman, A. T., & Anderegg, W. R. L. (2025). Data from: Betting on-rain: Stand structure and leaf area overshoot relate to increased tree mortality from drought. *Dryad Digital Repository*. https://doi.org/10.5061/dryad.vt4gbw83q

Kerr, K. L., Anderegg, L. D. L., Zenes, N., & Anderegg, W. R. L. (2022). Quantifying within-species trait variation in space and time reveals limits to trait-mediated drought response. *Functional Ecology*, *36*, 2399–2411.

Kuznetsova, A., Brockhoff, P. B., & Christensen, R. H. B. (2017). lmerTest package: Tests in linear mixed effects models. *Journal of Statistical Software*, *82*(13), 1–26. https://doi.org/10.18637/jss.v082.i13

Lachenbruch, B., St. Clair, J. B., & Harrington, C. A. (2021). Differences in branch hydraulic architecture related to the aridity of growing sites and seed sources of coastal Douglas-fir saplings. *Tree Physiology*, *42*(2), 351–364. https://doi.org/10.1093/treephys/tpab106

Lenth, R. V. (2022). emmeans: Estimated marginal means, aka least-squares means. *CRAN Repository*. https://CRAN.R-project.org/package=emmeans

Licor. (1992). *LAI-2000 plant canopy analyzer operating manual*. Licor.

Macinnis-Ng, C., McClenahan, K., & Eamus, D. (2004). Convergence in hydraulic architecture, water relations and primary productivity amongst habitats and across seasons in Sydney. *Functional Plant Biology*, *31*, 429–439.

Marchetti, S. B., Worrall, J. J., & Eager, T. (2011). Secondary insects and diseases contribute to sudden aspen decline in Southwestern Colorado, USA. *Canadian Journal of Forest Research*, *41*, 2315–2325.

Martin, J. G., Kloeppel, B. D., Schaefer, T. L., Kimbler, D. L., & McNulty, S. G. (1998). Aboveground biomass and nitrogen allocation of ten deciduous southern Appalachian tree species. *Canadian Journal of Forest Research*, *28*(11), 1648–1659. https://doi.org/10.1139/x98-146

Martínez-Vilalta, J., Cochard, H., Mencuccini, M., Sterck, F., Herrero, A., Korhonen, J. F. J., Llorens, P., Nikinmaa, E., Nolè, A., Poyatos, R., Ripullone, F., Sass-Klaassen, U., & Zweifel, R. (2009). Hydraulic adjustment of scots pine across Europe. *New Phytologist*, *184*, 353–364.

Martínez-Vilalta, J., Piñol, J., & Beven, K. (2002). A hydraulic model to predict drought-induced mortality in woody plants: An application to climate change in the Mediterranean. *Ecological Modelling*, *155*(2–3), 127–147. https://doi.org/10.1016/S0304-3800(02)00025-X

McBranch, N. A., Grossiord, C., Adams, H., Borrego, I., Collins, A. D., Dickman, T., Ryan, M., Sevanto, S., & McDowell, N. G. (2019). Lack of acclimation of leaf area: Sapwood area ratios in pinon pine and juniper in response to precipitation reduction and warming. *Tree Physiology*, *39*(1), 135–142. https://doi.org/10.1093/treephys/tpy066

McDowell, N., Barnard, H., Bond, B. J., Hinckley, T., Hubbard, R. M., Ishii, H., Köstner, B., Magnani, F., Marshall, J. D., Meinzer, F. C., Phillips, N., Ryan, M. G., & Whitehead, D. (2002). The relationship between tree height and leaf area: Sapwood area ratio. *Oecologia*, *132*, 12–20.

Meier, G. A., Brown, J. F., Evelsizer, R. R., & Worrall, J. J. (2015). Phenology and climate relationships in aspen (*Populus tremuloides* Michx.) forest and woodland communities in the San Juan Mountains of Colorado. *Ecological Indicators*, *48*, 189–197. https://doi.org/10.1016/j.ecolind.2014.05.033

Meinzer, F. C., Bond, B. J., Warren, J. M., & Woodruff, D. R. (2005). Does water transport scale universally with tree size? *Functional Ecology*, *19*, 558–565.

Meinzer, F. C., Goldstein, G., & Andrade, J. L. (2001). Regulation of water flux through tropical forest canopy trees: Do universal rules apply? *Tree Physiology*, *21*, 19–26.

Mencuccini, M. (2002). Hydraulic constraints in the functional scaling of trees. *Tree Physiology*, *22*, 553–565.

Mencuccini, M., & Grace, J. (1995). Climate influences the leaf area/sapwood area ratio in scots pine. *Tree Physiology*, *15*, 1–10.

Mencuccini, M., Rosas, T., Rowland, L., Choat, B., Cornelissen, J. H. C., Plavcová, L., Wright, I., Blackman, C. J., Gleason, S., Jansen, S., Kramer, K., Lapenis, A., Manzoni, S., Schwalm, C., Tissue, D., Wolfe, B., Zaehle, S., & Martínez-Vilalta, J. (2020). Leaf economics and plant hydraulics drive leaf: Wood area ratios. *New Phytologist*, *224*, 1544–1556.

Mitton, J. B., & Grant, M. C. (2003). Genetic variation and the natural history of quaking aspen. *BioScience*, *46*, 25–31.

Notaro, M., & Zarrin, A. (2011). Subseasonal variability and the North American monsoon to antecedent Rocky Mountain snowpack. *Geophysical Research Letters*, *38*, 1–6.

Pascale, S., Boos, W. R., Bordoni, S., Delworth, T. L., Kapnick, S. B., Murakami, H., Vecchi, G. A., & Zhang, W. (2017). Weakening of the North American monsoon with global warming. *Nature Climate Change*, *7*(11), 806–812. https://doi.org/10.1038/nclimate3412

R Core Team. (2021). *R: A language and environment for statistical computing*. R Foundation for Statistical Computing. https://www.R-project.org/

Refsland, T. K., & Cushman, J. H. (2021). Continent-wide synthesis of the long-term population dynamics of quaking aspen in the face of accelerating human impacts. *Oecologia*, *197*, 25–42.

Richardson, A. D., Keenan, T. F., Migliavacca, M., Ryu, Y., Sonnentag, O., & Toomey, M. (2013). Climate change, phenology, and phenological control of vegetation feedbacks to the climate system. *Agricultural and Forest Meterology*, *169*, 156–173. https://doi.org/10.1016/j.agrformet.2012.09.012

Rosas, T., Mencuccini, M., Barba, J., Cochard, H., Saura-Mas, S., & Martínez-Vilalta, J. (2019). Adjustments and coordination of hydraulic, leaf and stem traits along a water availability gradient. *New Phytologist*, *223*(2), 632–646. https://doi.org/10.1111/nph.15684

Sabot, M. E. B., De Kauwe, M. G., Pitman, A. J., Medlyn, B. E., Ellsworth, D. S., Martin-StPaul, N. K., Wu, J., Choat, B., Limousin, J.-M., Tissue, D. T., Rogers, A., & Serbin, S. P. (2022). One stomatal model to rule them all? Toward improved representation of carbon dynamics in vegetation models. *Journal of Advances in Modeling Earth Systems*, *14*(4), e2021MS002761. https://doi.org/10.1029/2021MS002761

Schneider, C. A., Rasband, W. S., & Eliceiri, K. W. (2012). NIH image to ImageJ: 25 years of image analysis. *Nature Methods*, *9*, 671–675.

Seager, R., Ting, M., Held, I., Kushnir, Y., Lu, J., Vecchi, G., Huang, H.-P., Harnik, N., Leetmaa, A., Lau, N.-C., Li, C., Velez, J., & Naik, N. (2007). Model projections of an imminent transition to a more arid climate in southwestern North America. *Science*, *316*(5828), 1181–1184. https://doi.org/10.1126/science.1139601

Shinozaki, K., Yoda, K., Hozumi, K., & Kira, T. (1964). A quantitative analysis of plant form—The pipe model theory I. Basic analyses. *Japanese Journal of Ecology*, *14*, 97–105.

Sperry, J. S., Donnelly, J. R., & Tyree, M. T. (1988). A method for measuring hydraulic conductivity and embolism in xylem. *Plant, Cell and Environment*, *11*(1), 35–40.

Sperry, J. S., Hacke, U. G., Oren, R., & Comstock, J. P. (2002). Water deficits and hydraulic limits to leaf water supply. *Plant, Cell and Environment*, *25*(2), 251–263. https://doi.org/10.1046/j.0016-8025.2001.00799.x

Trugman, A. T., Anderegg, L. D. L., Anderegg, W. R. L., Das, A. J., & Stephenson, N. L. (2021). Why is tree drought mortality so hard to predict? *Trends in Ecology & Evolution*, *36*(6), 520–532. https://doi.org/10.1016/j.tree.2021.02.001

Trugman, A. T., Anderegg, L. D. L., Wolfe, B. T., Birami, B., Ruehr, N. K., Detto, M., Bartlett, M. K., & Anderegg, W. R. L. (2020). Climate and plant trait strategies determine tree carbon allocation to leaves and mediate future forest productivity. *Global Change Biology*, *26*(10), 3896–3905. https://doi.org/10.1111/gcb.14680

Tsuruta, K., Ishida, A., Nakano, T., Tarumoto, M., Tanabe, H., Matsumoto, Y. (2000). Acclimation of photosynthesis to previous-year and current-year solar irradiance in *Abies mariesii*. *Tree Physiology*, *20*(14), 945–951. https://doi.org/10.1093/treephys/20.14.945

Williams, A. P., Cook, E. R., Smerdon, J. E., Cook, B. I., Abatzoglou, J. T., Bolles, K., Baek, S. H., Badger, A. M., & Livneh, B. (2020). Large contribution from anthropogenic warming to an emerging north American megadrought. *Science*, *368*(6488), 314–318. https://doi.org/10.1126/science.aaz9600

Wirth, R., Weber, B., & Ryel, R. J. (2001). Spatial and temporal variability of canopy structure in a tropical moist forest. *Acta Oecologica*, *22*, 235–244.

Worrall, J. J., Egeland, L., Eager, T., Mask, R. A., Johnson, E. W., Kemp, P. A., & Shepperd, W. D. (2008). Rapid mortality of *Populus tremuloides* in southwestern Colorado, USA. *Forest Ecology and Management*, *255*, 686–696.

Worrall, J. J., Marchetti, S. B., Egeland, L., Mask, R. A., Eager, T., & Howell, B. (2010). Effects and etiology of sudden aspen decline in southwestern Colorado, USA. *Forest Ecology and Management*, *260*, 638–648.

Wu, A., Anderegg, L. D. L., Dawson, T. E., & Trugman, A. T. (2023). Leaf trait coordination and variation of blue oak across topo-environmental scales. *Tree Physiology*, *43*, 2088–2103.

Wu, J., Serbin, S. P., Ely, K. S., Wolfe, B. T., Dickman, L. T., Grossiord, C., Wright, S. J., Collins, A. D., Rogers, A., Sloan, V. L., Wullschleger, S. D., Wang, H., Xu, C., McDowell, N. G., Martin, R. E., Kueppers, L. M., Koven, C. D., Knox, R. G., Walker, A. P., … Christoffersen, B. O. (2020). The response of stomatal conductance to seasonal drought in tropical forests. *Global Change Biology*, *26*(2), 823–839. https://doi.org/10.1111/gcb.14851

Xu, X., Medvigy, D., Powers, J. S., Becknell, J. M., & Guan, K. (2016). Diversity in plant hydraulic traits explains seasonal and inter-annual variations of vegetation dynamics in seasonally dry tropical forests. *New Phytologist*, *212*(1), 80–95. https://doi.org/10.1111/nph.14009

Yang, J., Tian, H., Pan, S., Chen, G., Zhang, B., & Dangal, S. (2018). Amazon drought and forest response: Largely reduced forest photosynthesis but slightly increased canopy greenness during the extreme drought of 2015/2016. *Global Change Biology*, *24*(5), 1919–1934. https://doi.org/10.1111/gcb.14056

Yang, J., Tian, H., Pan, S., Lu, C., Dangal, S. R. S., Tao, B., Xu, X., & Yang, Q. (2015). Amplified modulation of the monsoon intensity over the Indian subcontinent by atmospheric brown clouds: Possible local and remote forcings. *Journal of Geophysical Research: Atmospheres*, *120*(12), 6156–6175. https://doi.org/10.1002/2015JD023305

Yang, J., Tian, H., Pan, S., Lu, C., Xu, R., Woodward, F. I., Ren, W., Wang, Y., & Tai, X. (2019). The impact of rising CO_2 and acclimation on the response of US forests to global warming. *Proceedings of the National Academy of Sciences of the United States of America*, *116*, 25734–25744.

Zhang, J., Nielsen, S. E., Mao, L., & Chen, G. (2014). Energy, ecological constraints and historical factors supplement current climate in shaping global forest canopy height. *Journal of Ecology*, *104*(2), 469–478. https://doi.org/10.1111/1365-2745.12510

Zhang, Y., Keenan, T. F., & Zhou, S. (2021). Exogenous and endogenous controls of global land-surface water use efficiency. *Nature Ecology & Evolution*, *5*, 1490–1498.

Zhu, C., Lettenmaier, D. P., & Cavazos, T. (2005). Role of antecedent land surface conditions on North American monsoon rainfall variability. *Journal of Climate*, *18*, 3104–3121.

Zhu, L., & Zhao, P. (2023). Climate-driven sapwood-specific hydraulic productivity and the Huber value but not leaf-specific hydraulic conductivity on a global scale. *Science of the Total Environment*, *857*, 159334.

SUPPORTING INFORMATION

Additional supporting information can be found online in the Supporting Information section at the end of this article.

Table S1: Table of mean annual precipitation values (mm) for individual years of interest in the study. MAP represents the 1961–1990 climate normal. For each year in the table, the annual precipitation total is provided followed by the amount this total deviated from MAP (− means less precipitation, + means more precipitation compared to normal). Climate data were obtained from TerraClimate

Table S2: Characteristics of study plots. Plots for the within-forest portion of the study were established in the San Juan National Forest in 2014 and 2018. Plots for the across-forest portion of the study were established in five National Forests (Dixie, San Juan, Uncompahgre, White River, and Uinta National Forests) in 2020. Values represent means (and standard deviations) of plots in elevation zones (low (Low), middle (Mid) and high (High) elevation) within the San Juan National Forest (A), and across forests for all National Forests (B). Bracketed numbers indicate total number of plots in each zone/forest. Plots were predominately south-southwest facing (SW = southwest to S). Diameter at breast height (DBH) = mean values of all > 13 cm DBH aspen in the plots. Age = the average age of the trees in the plots estimated from tree ring data measured in 2014 (A), and tree ring data measured in 2020 (B).

Figure S1: Plots depict the relationships between diameter at breast height (DBH) and sapwood area for trees sampled (cored) from each National Forest (Dixie, San Juan, Uncompahgre, White River and Uinta). Power regression models were fit to each relationship, and model equations (printed at bottom right in corresponding colours to the forest) were used to estimate sapwood area for all trees in the study plots. Lines represent power regression model fits that have been coloured according to forest.

Figure S2: Plots depict the relationships between diameter at breast height (DBH) and basal area increment indexes of the eight most recent years of growth (BAI_8) for trees sampled (cored) from each National Forest (Dixie, San Juan, Uncompahgre, White River and Uinta). Linear regression models were fit to each relationship, and model equations (printed at bottom right in corresponding colours to the forest) were used to estimate BAI_8 for all trees in the study plots. Lines represent linear regression model fits that have been coloured according to forest, and shaded areas represent 95% confidence intervals.

Figure S3: Figure 3 (Main) and Figure S3 (Main) plot the ratio of most recent years of growth (LAI:BAI_8) indicated sapwood growth declines relative to leaf area in low elevations in the San Juan NF. (A) Stand-level LAI: BAI_8 was highest in the San Juan NF, stand-level LAI:BAI_8 was highest in low elevation aspen during the severe 2018 drought. In A, aspen populations have been arranged left to right according to the amount of summer monsoonal precipitation they receive (high to low), which also follows a south to north latitudinal gradient. Significant differences between elevation zones are indicated. For both panels, bars represent means and error bars represent 95% confidence intervals.

Figure S4: The 2018 drought (mean DBH loss) of conductance was near 50% precipitation, indicating elevated drought stress. Aspen populations have been arranged left to right according to the amount of summer monsoonal precipitation they receive (high to low), which also follows a south to north latitudinal gradient. Bars represent mean values. Uncompahgre, White River and Uinta. Lowercase letters indicate significant differences between the populations.

How to cite: Kerr, K. L., Anderegg, L. D. L., Trugman, A. T., & Anderegg, W. R. L. (2025). Betting on rains that do not come: Monsoon failure and relate to increased tree mortality from drought. *Functional Ecology*, *39*, 1840–1852. https://doi.org/10.1111/1365-2435.70054